Article

Not peer-reviewed version

# Alkaloid Profiling and Anti-Cholinesterase Potential of Three Different Genera of Amaryllidaceae Collected in Ecuador: *Urceolina* Rchb., *Clinanthus* Herb., and *Stenomesson* Herb

Luciana R. Tallini , Karen Acosta León , Raúl Chamorro , Edison H. Osorio , Jaume Bastida , Lou Jost , Nora H. Oleas *

Posted Date: 9 April 2024

doi: 10.20944/preprints202404.0592.v1

Keywords: Amaryllidoideae; alkaloids; Amazon lily; Alzheimer's disease; computational experiments

*Article*

# Alkaloid Profiling and Anti-Cholinesterase Potential of Three Different Genera of Amaryllidaceae Collected in Ecuador: *Urceolina* Rchb., *Clinanthus* Herb., and *Stenomesson* Herb

**Luciana R. Tallini [1], Karen Acosta León [2], Raúl Chamorro [2], Edison H. Osorio [3], Jaume Bastida [1], Lou Jost [4] and Nora H. Oleas [5,*]**

[1] Grup de Productes Naturals, Departament de Biologia, Sanitat i Medi Ambient, Facultat de Farmàcia i Ciències de l'Alimentació, Universitat de Barcelona, Av. Joan XXIII 27-31, 08028 Barcelona, Spain;
[2] Grupo de Investigación de Productos Naturales y Farmacia, Facultad de Ciencias, Escuela Superior Politécnica del Chimborazo, Panamericana Sur km 1 1/2, EC060155 Riobamba, Ecuador;
[3] Facultad de Ciencias Naturales y Matemáticas, Universidad de Ibagué, Carrera 22 calle 67, Ibagué, Colombia;
[4] Fundación Ecominga, Vía a Runtún s/n, Baños, Tungurahua, Ecuador;
[5] Centro de Investigación de la Biodiversidad y Cambio Climático (BioCamb) y Facultad de la Salud y Bienestar Humano, Universidad Tecnológica Indoamérica, Machala y Sabanilla, EC170301 Quito, Ecuador.
* Correspondence: noraoleas@uti.edu.ec

**Abstract:** Ecuador is an important center of biodiversity of the plant family Amaryllidaceae, specially the subfamily Amaryllidoideae, known as a source of important bioactive molecules. The aim of this study was to assess the chemical and biological potential of four different species of Amaryllidoideae collected in Ecuador: *Urceolina formosa*, *Urceolina ruthiana*, *Clinanthus incarnatus*, and *Stenomesson aurantiacum*. Sixteen alkaloids were identified in the bulb extract of these species by GC-MS, which the extract of *S. aurantiacum* exhibiting the greatest structural diversity. The potential of these three genera against Alzheimer's disease was evaluated by measuring their AChE and BuChE inhibitory activity, revealing that *C. incarnatus* and *U. formosa* (from Sucumbíos province) showed the best results with $IC_{50}$ values of 1.73 ± 0.25 and 30.56 ± 1.56 $\mu g \cdot ml^{-1}$, respectively. Molecular dynamic assays were conducted to elucidate the possible interactions that occurs among 2-hydroxyanhydrolycorine and AChE enzyme, suggesting some similarity with those observed for galanthamine. This study enhances our understanding of the biodiversity of Amaryllidoideae species from Ecuador, highlighting their potential as a source of chemical compounds with pharmaceutical potential.

**Keywords:** Amaryllidoideae; alkaloids; Amazon lily; Alzheimer's disease; computational experiments

## 1. Introduction

The Amaryllidaceae family, specifically the subfamily Amaryllidoideae, is an important source of an exclusive and still expanding group of alkaloids, known as Amaryllidaceae alkaloids, that shows a broad spectrum of biological activities [1]. This subfamily comprises ca. 900 species and 75 genera, bringing up about 700 Amaryllidaceae alkaloids, which are mainly classified into nine skeleton types, represented by norbelladine-, lycorine-, homolycorine-, crinine-, haemanthamine-, narciclasine-, tazettine-, montanine- and galanthamine-type structures [2,3].

The subfamily Amaryllidoideae is found in different zones, being South America, South Africa, and the Mediterranean region, the most representative [2]. Cultures worldwide have utilized Amaryllidaceae plants for centuries in traditional medicine, recognizing their pharmaceutical potential often linked to the production of specific alkaloids [4]. Ecuador is the major center of diversity in the tribe Eucharideae (Amaryllidaceae) [5], including the genus *Urceolina* Planch. This genus, known as Amazon lily, is mainly distributed in the western Amazon basin and the adjoining lower slopes of the eastern Andean cordillera [6]. The genus *Stenomesson* Herb. (Amaryllidaceae) is mainly found in Peru, with only *S. aurantiacum* Herb. previously reported in Ecuador [7]. These plants usually occur in seasonally dry, grassy vegetation or at the margins of cloud forests above 2000 m

 doi:10.20944/preprints202404.0592.v1



elevation, but are also found in Peruvian inter-Andean valleys below 2000 m [8], and in the loma formations along the coast of this country, being all the petiolate-leafed Stenomesseae more closely related to Eucharideae than to the lorate leafed Stenomesseae [5,9]. The genus *Clinanthus* Herb. (Amaryllidaceae), endemic to Peru and Ecuador [10], was separated from *Stenomesson*, and is primarily known in its same locations [8,11,12].

Regarding the traditional use of these plants, *Urceolina* species have been documented as compresses applied to sores and tumors by native people in Ecuador, and the Jíbaro indigenous people in Peru have utilized them for treating facial blemishes and acne [13]. Additionally, archeological findings at Inca ruins in South America suggest that certain Amaryllidaceae genera, such as *Stenomesson*, were depicted on ceremonial drinking vessels, and may have held significance within popular culture [8,14]. In recent years, the Amaryllidaceae species from Ecuador have garnered significant attention due to their alkaloid profiling and potential therapeutic benefits against Alzheimer's disease. The description and understanding of these species have progressively expanded in the literature in the last 10 years [15-18].

Dementia is a significant contributor to disability and dependency in the elderly population [19]. This condition gives rise to physical, psychological, social, and economic impacts, with Alzheimer's disease being the most prevalent form of this disorder [19]. The development of Alzheimer's disease appears to involve various mechanisms, one of which is a decrease in the neurotransmitter acetylcholine in the inter-synaptic space [20]. Currently, galanthamine, donepezil, and rivastigmine are the only cholinesterase inhibitor drugs approved by FDA for the clinical treatment of mild to moderate Alzheimer's disease symptomatology. The first one, galanthamine - an Amaryllidaceae alkaloid originally isolated from *Galanthus woronowii* in 1952, has been commercialized under its salt form since 2001 [21]. However, the synthesis of this molecule remains expensive, as pharmaceutical companies continue to obtain it from Amaryllidaceae species [22].

The aim of this study was to evaluate the chemical and biological potential of five samples of Amaryllidaceae collected in Ecuador. The alkaloid extracts from the bulbs of *Urceolina formosa* Meerow, *Urceolina ruthiana* L. Jost, Oleas & Meerow, *Clinanthus incarnatus* (Kunth) Meerow, and *Stenomesson aurantiacum* (Kunth) Herb. were analyzed using gas chromatography coupled to mass spectrometry (GC-MS). Additionally, their potential in combating Alzheimer's disease was estimated by evaluating their inhibitory activity against cholinesterase enzymes, acetylcholinesterase (AChE) and butyrylcholinesterase (BuChE). Computational experiments were also conducted to gain further insights into the molecular interactions among alkaloid-AChE.

## 2. Results and Discussion

### *2.1. Alkaloid Profile*

The alkaloid extracts of five samples of Amaryllidaceae collected in Ecuador were analyzed, resulting in the quantification of sixteen alkaloids. These molecules are listed in **Table 1** and visually represented in **Figure 1**. The quantities of each compound are reported in milligrams of galanthamine (mg GAL) per gram of alkaloid extract (g AE).

**Table 1.** Alkaloids identified in Amaryllidaceae species collected in Ecuador by GC-MS. Values are expressed as mg GAL·g$^{-1}$ AE.

| Alkaloid | RI | [M$^+$] | BP | A | B | C | D | E |
|---|---|---|---|---|---|---|---|---|
| trisphaeridine (**1**) | 2323.1 | 223 | 223 | - | - | - | - | 8.1 |
| galanthamine (**2**) | 2386.1 | 287 | 286 | 46.2 | 28.2 | - | - | 74.1 |
| sanguinine (**3**) | 2452.4 | 273 | 273 | - | - | - | - | 7.8 |
| unidentified (galanthamine-type)[1] (**4**) | 2474.4 | 287 | 286 | - | - | - | - | 24.0 |
| galanthindole (**5**) | 2535.0 | 281 | 281 | - | - | - | - | 15.8 |
| 8-*O*-demethylmaritidine (**6**) | 2539.9 | 273 | 273 | - | - | - | - | 6.1 |
| anhydrolycorine (**7**) | 2543.6 | 251 | 250 | - | - | - | 24.5 | - |
| augustine (**8**) | 2576.1 | 301 | 301 | - | - | - | - | 45.4 |
| kirkine (**9**) | 2590.1 | 273 | 252 | - | - | - | - | 23.1 |
| haemanthamine (**10**) | 2611.5 | 301 | 272 | 172.5 | 37.2 | 101.4 | - | - |

Preprints.org (www.preprints.org) | NOT PEER-REVIEWED | Posted: 9 April 2024 doi:10.20944/preprints202404.0592.v1



| | | | | | | | | |
|---|---|---|---|---|---|---|---|---|
| tazettine (**11**) | 2620.4 | 331 | 247 | - | - | 32.6 | - | - |
| 11,12-dehydroanhydrolycorine (**12**) | 2644.4 | 249 | 248 | - | - | - | - | 181.6 |
| 11-hydroxyvittatine (**13**) | 2679.4 | 287 | 258 | 16.9 | 9.8 | - | - | 108.1 |
| unidentified (pretazettine-type)[1] (**14**) | 2697.3 | 331 | 261 | - | - | - | - | 8.2 |
| lycorine (**15**) | 2716.5 | 287 | 226 | 251.6 | 273.9 | 168.1 | 149.9 | - |
| 2-hydroxyanhydrolycorine [2] (**16**) | 2891.6 | 267 | 266 | - | - | - | 60.2 | - |
| **Total** | | | | **487.2** | **349.1** | **302.1** | **234.6** | **502.3** |

[1] proposed alkaloid-type according to fragmentation pattern; [2] proposed alkaloid structure according to fragmentation pattern by [23]; **A:** *Urceolina formosa* (from Tungurahua province); **B:** *Urceolina formosa* (from Sucumbíos province); **C:** *Urceolina ruthiana*; **D:** *Clinanthus incarnatus*; **E:** *Stenomesson aurantiacum*.

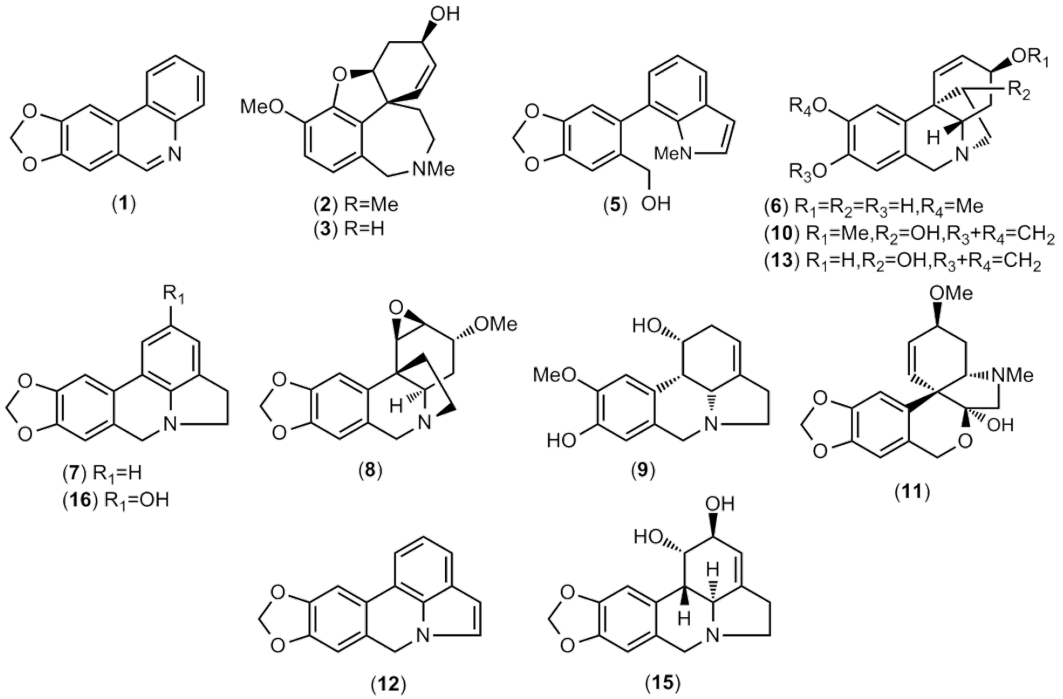


**Figure 1.** Structures of the alkaloids identified in Amaryllidaceae species collected in Ecuador.

Some similarities among the alkaloid profiling of the two samples of Ur*ceolina formosa* (collected in Tungurahua's and Sucumbíos' provinces) and *Urceolina ruthiana* have been observed in this scientific report (**Table 1**). All these samples showed the presence of alkaloids from haemanthamine- and lycorine-type skeleton in their chemical composition. The alkaloid haemanthamine (**10**) was reported in all the samples of *Urceolina* evaluated in this work, and presented a large abundance in *U. formosa* (sample B) and *U. ruthiana* (sample C), 172.5 and 101.4 mg GAL.g$^{-1}$ AE, respectively. The alkaloid 11-hydroxyvittatine (**13**) was found in both samples of *U. formosa* (samples A and B), but not in *U. ruthiana*. The alkaloid lycorine (**15**) also has been detected in all the extracts of *Urceolina* evaluated herein, being the highest concentration observed in the species *U. formosa* (from Sucumbíos province, sample B), followed by *U. formosa* (from Tungurahua province, sample A), with 273.9 and 251.6 mg GAL.g$^{-1}$ AE, respectively.

Galanthamine (**2**) was identified in the bulbs extract of both samples of *U. formosa* (sample A and B), being the highest amount in sample A, 46.2 mg GAL.g$^{-1}$ AE. The alkaloid tazettine (**11**), which belongs to pretazettine-type scaffolds, was reported only in the extract of *U. ruthiana*, 32.6 mg GAL.g$^{-1}$ AE. This compound is also known as 6-deoxytazzetine, which is an artifact from the alkaloid pretazettine [24]. No unidentified compound has been observed in the species of *Urceolina* evaluated herein (**Table 1**).

The alkaloid profiling of *Urceolina bonplandii* (published as *Eucharis bonplandii*) collected in Colombia showed the presence of structures from narciclasine-, galanthamine-, haemanthamine-,

 doi:10.20944/preprints202404.0592.v1



and lycorine-type scaffolds, comprising twelve Amaryllidaceae alkaloids, together with one unidentified compound [25,26]. The same authors also reported the alkaloid composition of *Urceolina caucana* (published as *Eucharis caucana*) collected in two different locations from Colombia - Risaralda and Chocó, describing the presence of structures belonging to narciclasine-, galanthamine-, and lycorine-type alkaloids in both samples, as well as structures from haemanthamine/crinine-, pretazettine-, and montanine-type which were observed just in the second species [25].

As shown in **Table 1**, *C. incarnatus* presented three alkaloids among its chemical profile, being lycorine (**15**) the most abundant (149.9 mg GAL·g$^{-1}$ AE). A great amount of the compound **16**, which must be identified as 2-hydroxyanhydrolycorine by Soto-Vásquez and co-workers [23], has been quantified in this species, 60 mg GAL·g$^{-1}$ AE (**Table 1**). According to the literature, *C. incarnatus* collected in Peru presented a high amount of lycorine (**15**), as well as seven other different alkaloids [27]. A current publication revealed the presence of two lycorine-type alkaloids in *C. incarnatus* collected in Ecuador, which are lycorine and 11,12-dehydroanhydrolycorine, and 4 unidentified structures, that probably belong to lycorine- and ismine-type skeleton [28].

According to **Table 1**, *Stenomesson aurantiacum*, sample E, showed the highest content of alkaloids, totalizing 502.3 mg GAL·g$^{-1}$ AE. Among the samples evaluated herein, this plant extract presented the most diversity of structures, totalizing 11 compounds, which two of them were not identified, **4** and **14**, and seem to belong to galanthamine- and pretazettine-type scaffold, respectively. The molecules 11,12-dehydroanhydrolycorine (**12**), 11-hydroxyvittatine (**13**), and galanthamine (**2**) were the most representative in this species, with 181.6, 108.1, and 74.1 mg GAL·g$^{-1}$ AE, respectively. Lycorine (**15**) has been quantified in all the samples evaluated in this work, except in *S. aurantiacum* (**Table 1**). In a previous work, 22 alkaloids were detected in *S. aurantiacum* collected in Ecuador, being haemanthamine the most abundant [15].

### *2.2. AChE and BuChE Inhibitory Activity*

The bulbs alkaloid extract of the five samples of Amaryllidaceae collected in Ecuador presented inhibitory activity against AChE and BuChE (**Figure 2**). The samples of *C. incarnatus* (sample D) and both samples of *U. formosa* (sample A and B) showed the best results toward AChE, with $IC_{50}$ values of 1.73 ± 0.25, 2.63 ± 0.83, and 2.81 ± 0.48 µg·ml$^{-1}$, respectively. The samples of *U. formosa* (sample A and B) presented the best results against BuChE, with $IC_{50}$ values of 34.22 ± 1.46 and 30.56 ± 1.56 µg·ml-1, respectively, while *C. incarnatus* (sample D) showed $IC_{50}$ values of 50.51 ± 3.93 µg·ml$^{-1}$ against this enzyme. The $IC_{50}$ values obtained with the alkaloid extract of *U. ruthiana* and *S. aurantiacum* against AChE were 8.15 ± 0.07 and 3.41 ± 0.05 µg·ml$^{-1}$, respectively, and 57.26 ± 1.69 and 81.60 ± 9.97 µg·ml$^{-1}$, respectively, against BuChE. Galanthamine was used as control and showed $IC_{50}$ values of 0.57 ± 0.05 and 3.77 ± 0.20 µg·ml$^{-1}$ against AChE and BuChE, respectively (**Figure 2**). As shown in Table 1, the presence of this alkaloid was observed in the bulbs extract of both samples of *U. formosa* (sample A and B), and *S. aurantiacum* (sample E), and it must be contributing for the cholinesterase inhibitory effect of these species.

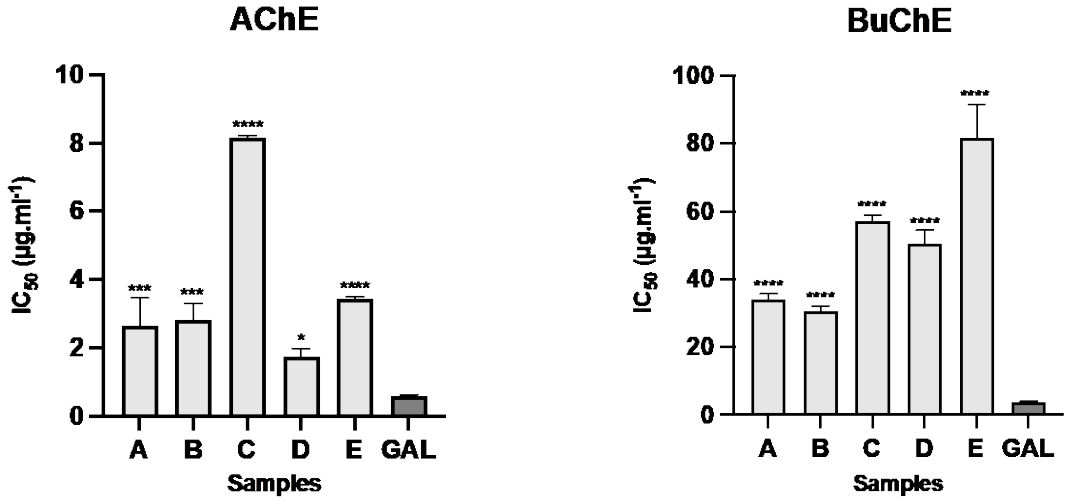

 doi:10.20944/preprints202404.0592.v1



**Figure 2.** AChE and BuChE inhibitory activity of different species of Amaryllidaceae collected in Ecuador. **A:** *Urceolina formosa* (from Tungurahua province); **B:** *Urceolina formosa* (from Sucumbíos province); **C:** *Urceolina ruthiana*; **D:** *Clinanthus incarnatus*; **E:** *Stenomesson aurantiacum*; **GAL:** galanthamine (control).

According to the literature, the bulbs extract of *U. bonplandii*, *U. caucana* (Risaralda) and *U. caucana* (Chocó) collected in Colombia showed $IC_{50}$ values lower than 10 μg·ml$^{-1}$ against the enzymes *Electrophorus electricus* and *human* AChE, and higher than 15 μg·ml$^{-1}$ against horse serum and human BuChE [26]. Among these samples, the authors reported that the best results were obtained with the bulbs extract of *U. bonplandii* which exhibited $IC_{50}$ values of 0.72 ± 0.05 μg·ml$^{-1}$ against hAChE [26]. Both leaves and bulbs extracts of *Urceolina bouchei* Woodson & P.H. Allen collected in Panama and evaluated by Calderón and co-authors showed activity against AChE though TLC bioautographic methodology, while the whole plant extract was inactive [29]. A currently publication described the $IC_{50}$ values of the alkaloid extract of *C. incarnatus* as higher than 40 μg·ml$^{-1}$ against AChE and BuChE, representing the low activity of this species against both enzymes [28]. Although the alkaloid profiling of *S. aurantiacum* have been previously reported in the literature, this is the first report about its anti-cholinestarase potential.

Previously works about six species of *Phaedranassa* (Amaryllidaceae) from Ecuador report their potential against Alzheimer's disease [16,17]. According to the literature, the species *P. cuencana* was the most active against AChE, with $IC_{50}$ values of 0.88 ± 0.11 μg·ml$^{-1}$, while the best activity against BuChE was observed for *P. dubia*, which showed $IC_{50}$ values of 14.26 ± 2.71 μg·ml$^{-1}$ [16,17]. Recently, the bulbs and leaves alkaloid extract of *Crinum* x *amabile* also collected in Ecuador have been evaluated against the same enzymes, being the bulbs the most active against AChE, with $IC_{50}$ values of 1.35 ± 0.13 μg·ml$^{-1}$, while the leaves showed better activity against BuChE, with $IC_{50}$ values of 8.50 ± 0.76 and 45.42 ± 3.72 μg·ml$^{-1}$, respectively [18].

### *2.3. Molecular Docking Results*

According to the results shown in **Table 1** and **Figure 2**, the species *C. incarnatus* presented a high concentration of the compound **16**, 2-hydroxyanhydrolycorine, and the best activity against AChE, respectively. Then, to know how **16** could work in the inhibition of this enzyme, a theoretical inhibition experiment was carried out through a molecular docking procedure using galantamine as a control. The *Tetronarce californica* AChE, a classical structure for biochemical studies of cholinergic neurotransmission [30,31], was used for all in-silico analysis. Molecular docking results provided binding energies for 2-hydroxyanhydrolycorine of -8.94 kcal·mol$^{-1}$ vs. galanthamine, -9.43 kcal·mol$^{-1}$. As a first approximation, our results indicate 2-hydroxyanhydrolycorine is not as active as galanthamine. Nevertheless, molecular docking data are only approximate and a molecular dynamics investigation must be performed to determine the true behavior within the active site of AChE.

The TcAChE protein's active site is about 20 nm deep and is composed by three important regions: (i) peripheral anionic site (PAS), which is composed predominantly by Tyr70, Tyr121, Asp72, Trp279 and Tyr334 residues, all located at the gate of the active site; ii) alpha-anionic site, place made up by Trp84 and Phe330 residues and are located in the middle of active site; and iii) catalytic anionic site (CAS), mainly constituted by Ser200, His440, and Glu 327 residues [32,33]. The ligand's position in TcAChE enzyme is reported in Figure 3. The 2-hydroxyanhydrolycorine molecule is located at the entrance of peripheral anionic site, PAS, and exhibits stabilizing interactions with Leu76, Trp86, Phe295, Tyr337, Tyr341 and Hsd447. Galantamine is located at the catalytic site bottom and shows stabilizing interactions with Trp86, Glu202, Ser203, Phe295, Tyr341, and Tyr337. Although 2-hydroxyanhydrolycorine and galanthamine inhibit differently the TcAChE, the results indicate that there are some residues which stabilize both ligands (Trp86, Phe295, Tyr337, Tyr341). Additionally, experimental reports have found synergistic effects of Amaryllidaceae alkaloids on inhibition of AChE, so this process could be carried out successfully [34].

 doi:10.20944/preprints202404.0592.v1



*2.3. Molecular dynamics (MD) simulations*

Molecular dynamics simulations were performed on the poses obtained by molecular docking experiments with the aim of elucidating how the structure 2-hydroxyanhydrolycorine could be inhibiting TcAChE. The free energy of binding for both complexes were performed using molecular mechanics generalized Born solvent accessibility (MM-GBSA). A small variation in root-mean-square deviation (RMSD) study indicates the stability of protein-ligand conformations during MD (Figure 4).

The binding free energies reported in Table 2 suggest 2-hydroxyanhydrolycorine complex is significantly less stable than galantamine complex at 13 kcal.mol$^{-1}$. These results were consistent with those obtained in molecular docking experiments and indicate that, although 2-hydroxyanhydrolycorine is not as active as galanthamine, it could be a potential inhibitor of TcAChE.

A frequency graph of contact between the most significant residues and 2-hydroxyanhydrolycorine and galantamine molecules along the MD is presented in Figure 4. A radius of 3 Å has been chosen due to this being the average distance between hydrogen bond variations in the analyzed systems. The MD results show galantamine remaining mostly in the bottom of the active site, near Asn87, Ser125, Gly126, Tyr133, Glu202, Ser203, and Phe295 residues, whereas 2-hydroxyanhydrolycorine is localized at the PAS site near to Leu76, Thr83, Tyr77, Trp286, Ser293, Val294, Glu334, Phe338, and Pro446 residues. Finally, Figure 5 shows both ligands have a significant frequency of contact with Phe297 residue, which is involved in the formation of the acyl-binding pocket.

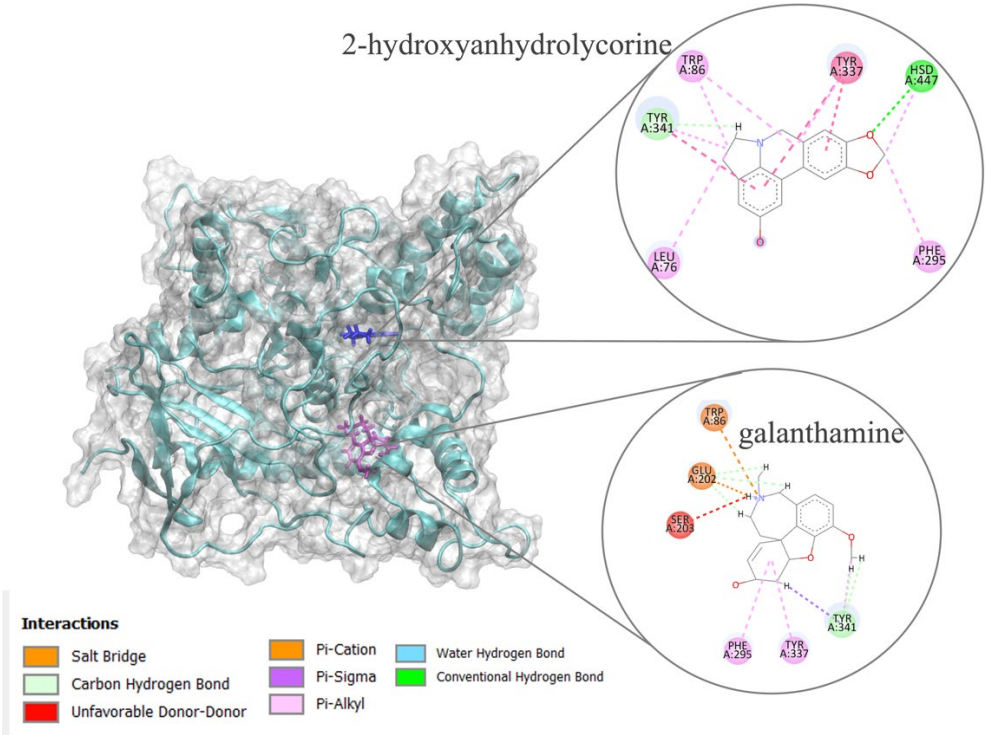


**Figure 3.** Ligand conformations in the TcAChE enzyme obtained by molecular docking experiments.

 doi:10.20944/preprints202404.0592.v1



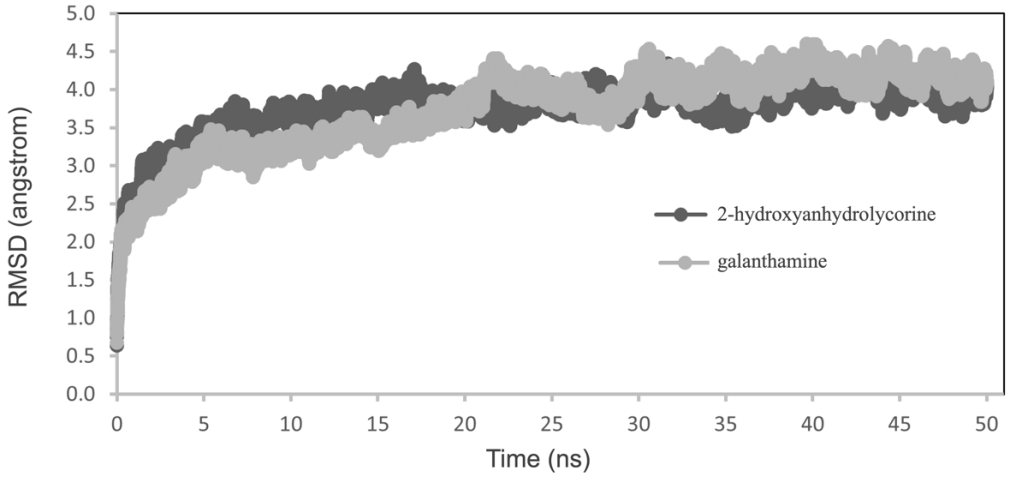


**Figure 4.** RMSD analysis for 2-hydroxyanhydrolycorine-TcAChE and galanthamine- TcAChE complexes.

**Table 2.** Free energy calculations of ligand-TcAChE complexes calculated through molecular dynamics and molecular docking procedures.

| **Substrate** | **MM-GBSA (kcal·mol$^{-1}$)*** | **Molecular Docking (kcal·mol$^{-1}$)** |
|---|---|---|
| 2-hydroxyanhydrolycorine | -23.695 (2.106) | -8.94 |
| galanthamine | -36.710 (2.842) | -9.43 |

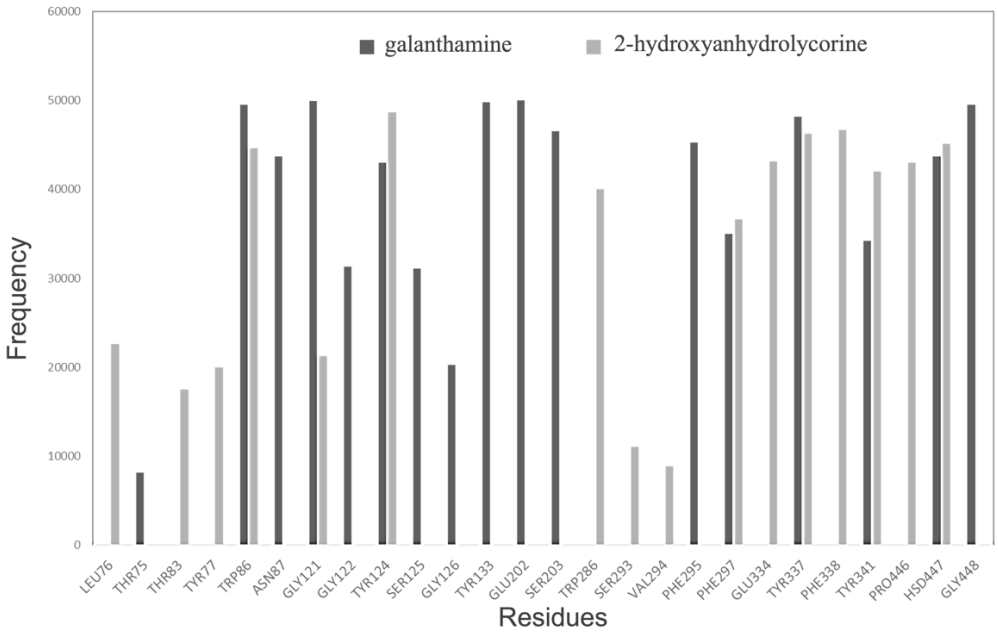


**Figure 5.** Residue occurrence frequencies at 3 Å or less from the ligand within the ligand-TcAChE complex calculated by molecular dynamics procedures.

## 3. Materials and Methods

### *3.1. Plant Material*

Five samples of Amaryllidaceae have been evaluated in this study, all of them collected in Ecuador in 2019 (Figures 6 and 7). *Urceolina formosa* (Ravenna) Ravenna (sample A) was collected at

 doi:10.20944/preprints202404.0592.v1



Sucumbíos province, at Cantón Shushufindi, Recinto el Mirador, kilometer 5, Ecuador. *Urceolina formosa* (Ravenna) Ravenna (sample B) was collected at Tungurahua province at Reserva Rio Zuñag. *Urceolina ruthiana* L. Jost, Oleas & Meerow (sample C) was obtained from Zamora-Chinchipe province, Copalinga private reserve, near Zamora. *Clinanthus incarnatus* (Kunth) Meerow (sample D) was collected at Chimborazo province, Guasuntos Panamericana highway. *Stenomesson aurantiacum* (Kunth) Herb. (sample E) was collected at Loja Province, close to the limit to Azuay. The species were authenticated by Alan Meerow from Arizona State University, USA.

### 3.2. Alkaloid Extraction

The bulbs of *Urceolina*, *Clinanthus*, and *Stenomesson* species were dried at 40 °C for 7 days. Then, the samples were triturated, and their powder was macerated with methanol at room temperature for 3 days, changing the solvent daily (3 × 100 mL), and, trying to increase the extraction potential, and ultrasonic baths was applied for 20 min, 8 times per day. The mash was filtered and evaporated to dryness under reduced pressure. The crude extracts of the bulbs were acidified with an aqueous solution of sulfuric acid (2%, *v*/*v*) to pH 2 and, then cleaned with diethyl ether to remove neutral material. The aqueous solution was basified with ammonium hydroxide at 25% (*v*/*v*) to pH 9–10 and extracted with ethyl acetate to obtain the alkaloid extract (AE) of each sample.

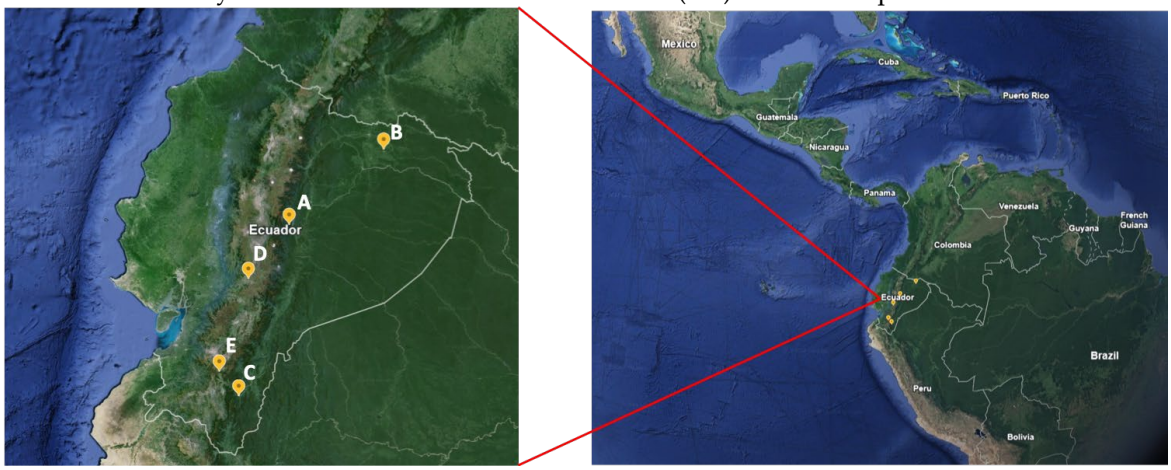


**Figure 6.** Map of Ecuador showing the sites of the samples. **A:** *Urceolina formosa* (from Tungurahua province); **B:** *Urceolina formosa* (from Sucumbíos province); **C:** *Urceolina ruthiana*; **D:** *Clinanthus incarnatus*; **E:** *Stenomesson aurantiacum*. Map source: Google Earth.

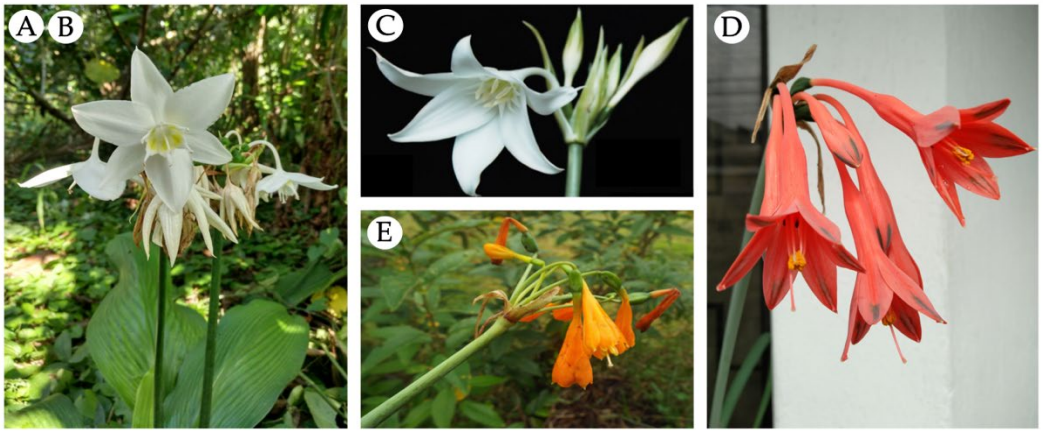


**Figure 7.** Flowering Amaryllidaceae species collected in Ecuador. **A, B**: *Urceolina formosa*; **C:** *Urceolina ruthiana*; **D:** *Clinanthus incarnatus*; **E:** *Stenomesson aurantiacum*. Pictures source: Nora H. Oleas.

### 3.3. GC-MS Analysis

 doi:10.20944/preprints202404.0592.v1



Two mg of each sample were dissolved in 1 ml of methanol: chloroform (0.5:0.5, *v*/*v*) and evaluated using GC-MS (Agilent Technologies 6890N coupled with MSD5975 inert XL; Santa Clara, CA, USA) equipment operating in electron ionization (EI) mode at 70 eV. A Sapiens-X5 MS column (30 m × 0.25 mm i.d., film thickness 0.25 µm; Teknokroma, Barcelona, Spain) was used. One µL of each sample was injected into the equipment using the splitless mode. Codeine (0.05 $mg.ml^{-1}$) was used as the internal standard. The injector and detector temperatures were 250 and 280 °C, respectively, and the flow-rate of carrier gas (He) was 1 $ml.min^{-1}$. The temperature gradient was 12 min at 100 °C, 100–180 °C at 15 °C·$min^{-1}$, 180–300 °C at 5 °C·$min^{-1}$, and 10 min hold at 300 °C.

A calibration curve of galanthamine (10, 20, 40, 60, 80, and 100 $\mu g.ml^{-1}$ was applied to quantify every single constituent detected in the chromatogram, using codeine (0.05 mg·$ml^{-1}$) as the internal standard. Peak areas were manually obtained, considering selected ions for each compound (usually the base peak of their MS, i.e., *m*/*z* at 286 for galanthamine and 299 for codeine). The ratio between the values obtained for galanthamine and codeine in each solution was plotted against the corresponding concentration of galanthamine to obtain the calibration curve and its equation ($y = 0.0112x - 0.0469$; $R^2 = 0.9995$). All data were standardized to the area of the internal standard (codeine), and the equation obtained for the calibration curve of galanthamine was used to calculate the amount of each alkaloid. Results are presented as mg GAL (galanthamine), which was finally related to the alkaloid extract (AE). As the peak area does not only depend on the corresponding alkaloid concentration but also on the intensity of the mass spectra fragmentation, the quantification is not absolute, but it is considered suitable to compare the specific alkaloid amount in Amaryllidaceae samples [35].

### *3.4. AChE and BuChE Inhibitory Activity*

Cholinesterases inhibitory activities were determined according to Ellman and co-workers [36] with some modifications as by López and co-workers [37]. Stock solutions with 500U of AChE from *Electrophorus electricus* (Merck, Darmstadt, Germany) and BuChE from equine serum (Merck, Darmstadt, Germany), respectively, were prepared and kept at −20 °C. Acetylthiocholine iodide (ATCI), S-butyrylthiocholine iodide (BTCI), and 5,50-dithiobis (2-nitrobenzoic) acid (DTNB) were obtained from Merck (Darmstadt, Germany). Fifty microliters of AChE or BuChE in phosphate buffer (8 mM $K_2HPO_4$, 2.3 mM $NaH_2PO_4$, 0.15 NaCl, pH 7.5) and 50 µl of the sample dissolved in the same buffer were added to the wells. The plates were incubated for 30 min at room temperature. Then, 100 µl of the substrate solution (0.1 M $Na_2HPO_4$, 0.5 M DTNB, and 0.6 mM ATCI or 0.24 mM BTCI in Millipore water, pH 7.5) was added. These reagents were obtained from Merck (Darmstadt, Germany). After 10 min, the absorbance was read at 405 nm in a Labsystem microplate reader (Helsinki, Finland). Enzymes activities were calculated as percent compared to a control using a buffer without any inhibitor. Galanthamine served as a positive control. In the first step, the activities of each sample against AChE and BuChE were assessed at 10, 100, and 200 µg·$ml^{-1}$. Then, the calibration curves of bulbs alkaloid extracts of *Urceolina*, *Clinanthus*, and *Stenomesson* species towards both enzymes were calculated and applied to obtain $IC_{50}$ values. The cholinesterase inhibitory data were analyzed with the Prism 10 software.

### *3.5. Statistical Analysis*

Three independent assays were used to evaluate the cholinesterase activity of the alkaloid extracts from the Amaryllidaceae species collected in Ecuador. Results were analyzed by ANOVA, using the Prism 10 software. Data are expressed as the mean ± standard deviation (SD). Significant results are marked as follows: **** $p < 0.0001$ and ** $p < 0.01$. For AChE and BuChE, one-way ANOVA with Dunnett's multiple comparison test was used to compare the mean of each column with the mean of a control column (galanthamine).

### *3.5. Molecular docking*

 doi:10.20944/preprints202404.0592.v1



The binding mechanisms of 2-hydroxyanhydrolycorine galantamine alkaloids to the active site in *Torpedo californica* acetylcholinesterase (TcAChE) protein, PDB code 1DX6 [38], were investigated using the AutoDock v.4.2 tool [39]. The use of TcAChE protein has been reported as a good instrument in the search for new cholinesterase inhibitors [40]. As a protein preparation procedure for the molecular docking experiment water, cofactors, and ions were removed from X-ray crystallographic structure. The polar hydrogen atoms were added, the atomic charges computed toward the Gasteiger procedure, and the non-polar hydrogen atoms merged. The grid maps required by AutoDock were computed using the auxiliary program AutoGrid, choosing a 60 Å × 60 Å × 60 Å grid box around the active site. The Lamarckian Genetic Algorithm (LGA) was used to conduct the docking searches [41] using 2000 individuals as a population, obtaining 2,500,000 energy evaluations for each 100 LGA run. The best docking complex poses were analyzed according to intermolecular interactions (ligand/enzyme), such as hydrogen bonding, hydrophobic interactions, and the cation–π, π–π stacking.

### *3.5. Molecular dynamics simulations (MD)*

MD experiments were achieved on the ligand-TcAChE (PDBID:1DX6) complex, in aqueous solutions with galantamine and 2-hydroxyanhydrolycorine as ligands employing TIP3P water model as an explicit solvent [42] (≈16.000 water molecules). Also, Na+ and Cl- ions were added to neutralize the systems and remain an ionic concentration of 0.15 mol·L$^{-1}$. A general AMBER force field (GAFF) has been used to parametrize galantamine and 2-hydroxyanhydrolycorine molecules [43,44]. The protein structure was modeled with CHARMM27 par_all27_prot_lipid.inp parameter [45]. The simulations were carried out using a standard MD protocol as follows: (I) minimization and structural relaxation of water molecules utilizing 2000 stages of minimization (downward step) and MD simulations with an NPT (310 K) assembly by 1000 ps employing harmonic constraints of 10 kcal·mol Å-2 on the protein and ligand; (II) minimization of the complete structure considering 2000 downstream minimization steps and 6500 steps of conjugate gradient minimization; (III) the minimized systems were progressively heated to 310 K, with harmonic restrictions of 10 kcal·mol Å$^{-2}$ in the carbon skeleton and ligand during 0.5 ns; (IV) The system was then balanced for 0.5 ns while adhering to the constraints, and then for 5 ns without constraints to 310 K in a canonical assembly (NVT); and (V) a production dynamic was conducted for 50 ns without constraints at 310 K and 1 atm with a temporary passage of 2 fs using an isothermal isobaric assembly (NPT). In the MD simulation, the temperature was controlled by the Langevin dynamics with a collision frequency of 1 ps$^{-1}$ (NVT) and the pressure with the Berendsen barostat (NPT). In addition, the Particle Mesh Ewald (PME) method with a cut-off value of 10 Å was used to treat nonbonding and long-range electrostatic interactions. All MD simulation calculations were performed using NAMD, software developed by the Theoretical and Computational Biophysics Group in the Beckman Institute for Advanced Science and Technology at the University of Illinois at Urbana-Champaign [46,47]. Molecular visualization of the systems and MD trajectory analysis were carried out with the VMD software package [48].

#### 3.5.1. Free energy calculations

The binding free energy of TcAChE-ligand complexes was estimated using the molecular MM/GBSA technique. For computations, the first 40 ns of MD were isolated and the explicit water molecules and ions were deleted. Three subsets of each system were analyzed using MM/ GBSA: the protein alone, the ligand alone, and the complex (protein-ligand). The total free energy (ΔGtot) was computed as follows for each of these subsets:

$$\Delta G = E_{MM} + G_{Solv} + T\Delta S_{conf}$$

Where EMM denotes the bonded and Lennard–Jones energy components; GSolv denotes the polar and nonpolar contributions to the solvation energy, respectively; T denotes the temperature; and ΔSconf denotes the conformational entropy [49]. Both EMM and GSolv were calculated using

 doi:10.20944/preprints202404.0592.v1



NAMD program with the generalized Born implicit solvent model [50]. ΔGtot was calculated as a linear function of the solvent-accessible surface area, which was calculated with a probe radius of 1.4 Å [51]. The difference between the binding free energies of TcACh and ligand complexes (ΔGbind) was used to compute the binding free energy of TcACh and ligand complexes (ΔGbind) where values represent the simulation's averages.

$$\Delta G_{bind} = G_{tot}(complex) + G_{tot}(protein) + G_{tot}(ligand)$$

## 4. Conclusions

In summary, this study was the first report about the alkaloid profiling of *Urceolina* species collected in Ecuador, as well as the first work about the anti-cholinesterase potential of the species studied herein, excepted *C. incarnatus*. The extract of *Stenomesson aurantiacum* presented unidentified structures among its profiling, suggesting this species as a possible source of new Amaryllidaceae alkaloids. The samples *C. incarnatus* and *Urceolina formosa* (collected in Sucumbíos province) provided the best results against AChE and BuChE, respectively. Computational experiments suggest some similarity in the interactions observed among 2-hydroxyanhydrolycorine and TcAChE with those observed for galanthamine. In vitro assays with 2-hydroxyanhydrolycorine must be carried out to corroborate the in silico findings. Our results highlight the importance of Amaryllidaceae species in the search of new bioactive molecules.

**Author Contributions:** Conceptualization, L.R.T. and N.H.O.; methodology, L.R.T., K.A.L., R.C., and E.H.O.; software, L.R.T. and E.H.O.; validation, E.H.O.; formal analysis, L.R:T., R.C., and E.H.O.; investigation, L.R.T. and E.H.O.; resources, K.A.L., E.H.O., J.B., and N.H.O.; data curation, L.R.T., K.A.L., and E.H.O.; writing—original draft preparation, L.R.T., E.H.O., and N.H.O.; writing—review and editing, K.A.L. and J.B.; visualization, L.J.; supervision, N.H.O.; project administration, J.B. and N.H.O.; funding acquisition, N.H.O. All authors have read and agreed to the published version of the manuscript.

**Funding:** This research was funded by Programa CYTED, grant number, 416RT0511 and Universidad TecnológicaIndoamérica, grant number Biocamb-02-(2016–2020). and "The APC was funded by Universidad Indoamérica Grant number INV-0019-003-006 ".

**Data Availability Statement:** Data is contained within the article.

**Acknowledgments:** The authors thank the Programa Iberoamericano de Ciencia y Tecnología para el Desarrollo (CYTED, 223RT0140) for providing the framework and economic support. L.R.T. and J.B. thank CCiTUB for technical support. The authors thank the Ministerio del Ambiente of Ecuador for collecting permits MAE-DNB-CM-2018-0086.

**Conflicts of Interest:** The authors declare no conflict of interest.

## References

1. Bastida, J.; Lavilla, R.; Viladomat, F. Chemical and biological aspects of *Narcissus* alkaloids. In: Cordell GA (ed), The Alkaloids: Chemistry and Physiology. 63, Elsevier, 2006, Amsterdam, pp. 87–179.
2. Berkov S, Osorio E, Viladomat F, Bastida J (2020) Chemodiversity, chemotaxonomy and chemoecology of AA. In: Knölker H-J (ed), The Alkaloids: Chemistry and Biology. 83, Elsevier, Amsterdam, pp. 113–185. https://doi.org/10.1016/bs.alkal.2019.10.002
3. Meerow, A.W.; Gardner, E.M.; Nakamura, K. Phylogenomicsof the Andean Tetraploid Clade of theAmerican Amaryllidaceae (SubfamilyAmaryllidoideae): Unlockinga Polyploid Generic Radiation Abettedby Continental Geodynamics. *Front. Plant Sci.* **2020**, *11*, 582422. https://doi.org/10.3389/fpls.2020.5824225.
4. Kornienko, A.; Evidente, A. Chemistry, biology and medicinal potential of narciclasine and its congeners. Chem. Rev. 2008, 108, 1982–2014. https://doi.org/10.1021/cr078198u
5. Meerow, A.W.; Jost, L.; Oleas, N. Two new species of endemic Ecuadorean Amaryllidaceae (Asparagales,Amaryllidaceae, Amarylloideae, Eucharideae). *Phytokeys* **2015**, *48*, 1-9. https://doi.org/10.3897/phytokeys.48.4399
6. Meerow, A.W. Biosyntematics of two sympatric species of *Eucharis* (Amaryllidaceae). *Pl Syst Evol* **1989**, *166*, 11-30.
7. Meerow, A.W. 202. Amaryllidaceae. In: Harling G, Andersson L (Eds) Flora of Ecuador 41: 1–52. Univ. Göteborg/Riksmuseum, Stockholm/Pontificia Univ. Católica del Ecuador, Quito, 1990.

8. Meerow, A.W.; Werff, H. van der. *Pucara* (Amaryllidaceae) Reduced to Synonymy with *Stenomesson* on the Basis of Nuclear and Plastid DNA Spacer Sequences, and a New Related Species of *Stenomesson*. *Syst. Bot.*, **2004**, *29:3*, 511-517; https://doi.org/10.1600/0363644041744400
9. Meerow, A.W.; Guy, C.L.; Li, Q-B.; Yang, S-L. Phylogeny of he American Amaryllidaceae based on nrDNA ITS sequences. *Syst. Bot.* **2000**, *25:4*, 708-726. https://doi.org/10.2307/2666729
10. Alzate, F.; Lesmes, M.; Cortés, N.; Varela, S.; Osorio, E. Sinopsis de la família Amaryllidaceae em Colombia. *Biota Colombiana*, **2019**, *20:1*, 1-20.
11. León, B.; Sagástegui, A.; Sánchez, I.; Zapata, M.; Meerow, A.; Cano, A. Amaryllidaceae endémicas del Perú. *Rev. Peru. Biol.*, **2006**, *13:2*, 690-697. ISSN 1727-9933
12. Leiva, S.; Meerow, A.W. A new species of *Clinanthus* from northern Peru (Asparagales, Amaryllidaceae, Amarylloideae, Clinantheae). *PhytoKeys*, **2016**, *63*, 99-106. https://doi.org/10.3897/phytokeys.63.8895
13. Cabezas, F.; Ramírez, A.; Viladomat, F.; Codina, C.; Bastida, J. Alkaloids from *Eucharis amazonica* (Amaryllidaceae). *Chem Pharm Bull* **2003**, *51:3*, 315-317.
14. Vargas, C.C. Phytomorphic representations of the ancient Peruvians. *Econ. Bot.* **1962**, *16*, 106-115. https://doi.org/10.1007/BF02985298
15. Acosta, K.; Pigni, N.; Oleas, N.; Bastida, J. Identification of the alkaloids of *Steno- messon aurantiacum* (Kunth) Herb., an Amaryllidaceae species from the Ecuadorian Andes. *PharmacologyOnline* **2014**, *3*, 178–183.
16. Acosta, K.; Inca, A.; Tallini, L.R.; Osorio, E.H.; Robles, J.; Bastida, J.; Oleas, N.H. Alkaloids of *Phaedranassa dubia* (Kunth) J.F. Macbr. and *Phaedranassa brevifolia* Meerow (Amaryllidaceae) from Ecuador and its cholinesterase-inhibitory activity. *S Afri J Bot* **2021**, *136*, 91-99. Doi: 10.1016/j.sajb.2020.09.007
17. Moreno, R.; Tallini, L.R.; Salazar, C.; Osorio, E.H.; Montero, E.; Bastida, J.; Oleas, N.H.; León, K.A. Chemical profiling and cholinesterase inhibitory activity of five *Phaedranassa* Herb. (Amaryllidaceae) species from Ecuador. *Molecules* **2020**, *25*, 2092. https://doi.org/10.3390/molecules25092092
18. Tallini, L.R.; Carrasco, A.; Acosta, K.L.; Vinueza, D.; Bastida, J.; Oleas, N.H. Alkaloid Profiling and Cholinesterase Inhibitory Potential of *Crinum* × *amabile* Donn. (Amaryllidaceae) Collected in Ecuador. *Plants* **2021**, *10*, 2686. https://doi.org/10.3390/plants10122686
19. WHO, 2023. Acessible online: https://www.who.int/health-topics/dementia#tab=tab_1 Accessed on 20 Nov, 2023.
20. Konrath, E.L.; dos Santos, C.P.; Klein-Júnior, L.C.; Henriques, A.T. Alkaloids as a source of potential anticholinesterase inhibitors for the treatment of Alzheimer's disease. *J. Pharm. Pharm.* **2013**, *65*, 1701–1725. https://doi.org/10.1111/jphp.12090
21. Berkov, S.; Georgieva, L.; Kondakova, V.; Atanassov, A.; Viladomat, F.; Bastida, J.; Codina, C. Plant sources of galanthamine: Phytochemical and biotechnological aspects. *Biotechnol. Biotechnol. Equip*. **2009**, *23*, 1170–1176. https://doi.org/10.1080/13102818.2009.10817633
22. Berkov, S.; Georgieva, L.; Sidjimova, B.; Bastida, J. Evaluation of *Hippeastrum papilio* (Ravenna) Van Scheepen potencial as a new industrial source of galanthamine. *Ind. Crop. Prod.*, **2022**, *178*, 114619. https://doi.org/10.1016/j.indcrop.2022.114619
23. Soto-Vásquez, M.R.; Alvarado-García, P.A.A.; Osorio, E.H.; Tallini, L.R.; Bastida, J. Antileishmanial activity of *Clinanthus milagroanthus* S. Leiva & Meerow (Amaryllidaceae) collected in Peru. *Plants*, **2023**, *12*, 322. https://doi.org/10.3390/plants12020322
24. de Andrade, J.P.; Pigni, N.B.; Torras-Claveria, L.; Berkov, S.; Codina, C.; Viladomat, F.; Bastida, J. Bioactive alkaloid extracts from *Narcissus broussonetii*: mass spectral studies. *J Pharmaceut Biomed* **2012**, *70*, 13-25. https://doi.org/10.1016/j.jpba.2012.05.009
25. Cortes, N.; Castañeda, C.; Osorio, E.H.; Cardona-Gomez, G.P.; Osorio, E. Amaryllidaceae alkaloids as agents with protective effects against oxidative neural cell injury. *Life Sci.* **2018**, *203*, 54-65. https://doi.org/10.1016/j.lfs.2018.04.026
26. Cortes, N.; Sierra, K.; Alzate, F.; Osorio, E.H.; Osorio, E. Alkaloids of Amaryllidaceae as Inhibitors of Cholinesterases (AChEs and BChEs): An Integrated Bioguided Study. *Phytochem Anal* **2018**, *29:2*, 217-227. https://doi.org/10.1002/pca.2736
27. Soto-Vásquez, M.R.; Horna-Pinedo, M.V.; Tallini, L.R.; Bastida, J. Chemical Composition and In Vitro Antiplasmodial Activity of the Total Alkaloids of the Bulbs of Two Amaryllidaceae Species from Northern Peru. *Pharmacogn. J.* **2021**, *13*, 1046–1052. https://doi.org/10.5530/pj.2021.13.135
28. Rodríguez-Escobar, M.L.; Tallini, L.R.; Lisa-Molina, J.; Berkov, S.; Viladomat, F.; Meerow, A.; Bastida, J.; Torras-Claveria, L. Chemical and Biological Aspects of Different Species of the Genus *Clinanthus* Herb. (Amaryllidaceae) from South America. *Molecules* **2023**, *28*, 5408. https://doi.org/10.3390/molecules28145408
29. Calderón, A.I.; Cubilla, M.; Espinosa, A.; Gupta, M.P. Screening of plants of Amaryllidaceae and related families from Panama as sources of acetylcholinesterase inhibitors. *Pharmaceutical Biology* **2010**, *48:9*, 988-993.
30. Lindstrom, J.; Cooper, J.; Tzartos, S. Acetylcholine receptors from *Torpedo* and *Electrophorus* have similar subunit structures. *Biochemistry* **1980**, *19:7*, 1454–1458. https://doi.org/10.1021/bi00548a029

31. Stavrianakou, M.; Perez, R.; Wu, C.; Sachs, M.S.; Aramayo, R.; Harlow, M. Draft de novo transcriptome assembly and proteome characterization of the electric lobe of *Tetronarce californica*: a molecular tool for the study of cholinergic neurotransmission in the electric organ. *BCM Genomics* **2017**, *18*, 611. https://doi.org/10.1186/s12864-017-3890-4
32. Silman, I.; Sussman, J.L. Acetylcholinesterase: How is structure related to function? *Chem-Biol. Interact*. **2008**, *175*, 3-10. https://doi.org/10.1016/j.cbi.2008.05.035
33. Dvir, H.; Silman, I.; Harel, M.; Rosenberry, T.L.; Sussman, J.L. Acetylcholinesterase: From 3D structure to function. *Chem-Biol. Interact.* **2010**, *187*, 10-22. https://doi.org/10.1016/j.cbi.2010.01.042
34. Orhan, I.; Sener, B. Bioactivity-directed fractionation of alkaloids from some Amaryllidaceae plants and their anticholinesterase activity. *Chem. Nat. Compd.* **2003**, *39*, 383–386. https://doi.org/10.1023/B:CONC.0000003421.65467.9c
35. Torras-Claveria, L.; Berkov, S.; Codina, C.; Viladomat, F.; Bastida, J. Metabolomic analysis of bioactive Amaryllidaceae alkaloids of ornamental varieties of *Narcissus* by GC-MS combined with k-means cluster analysis. *Ind. Crop. Prod.* **2014**, *56*, 211–222. https://doi.org/10.1016/j.indcrop.2014.03.008
36. Ellman, G.L.; Courtney, K.D.; Andres, Jr.V.; Featherstone, R.M. A new and rapid colorimetric determination of acetylcholinesterase activity. *Biochem. Pharm.* **1961**, *7*, 88–95. https://doi.org/10.1016/0006-2952(61)90145-9
37. López, S.; Bastida, J.; Viladomat, F.; Codina, C. Acetylcholinesterase inhibitory activity of some Amaryllidaceae alkaloids and *Narcissus* extracts. *Life Sci.* **2002**, *71*, 2521–2529. https://doi.org/10.1016/s0024-3205(02)02034-9
38. Greenblatt, H.M.; Kryger, G.; Lewis, T.; Silman, I.; Sussman, J.L. Structure of acetylcholinesterase complexed with (-)galanthamine at 2.3 Å resolution. FEBS Lett. 1999, 463, 321-326. https://doi.org/10.1016/s0014-5793(99)01637-3
39. Morris, G.M.; Huey, R.; Lindstrom, W.; Sanner, M.F.; Belew, R.K.; Goodsell, D.S.; Olson, A.J. AutoDock4 and AutoDockTools4: Automated Docking with Selective Receptor Flexibility. *J. Comput. Chem.* **2009**, *30:16*, 2785-2791. https://doi.org/10.1002/jcc.21256
40. Sierra, K.; de Andrade, J.P.; Tallini, L.R.; Osorio, E.H.; Yañéz, O.; Osorio, M.I.; Oleas, N.H.; García-Beltrán, O.; Borges, W. de S.; Bastida, J.; Osorio, E.; Cortes, N. *In vitro* and *in silico* analysis of galanthine from *Zephyranthes carinata* as an inhibitor of acetylcholinesterase. *Biomed. Pharmacother.* **2022**, *150*, 113016. https://doi.org/10.1016/j.biopha.2022.113016
41. Morris, G.M.; Goodsell, D.S.; Halliday, R.S.; Huey, R.; Hart, W.E.; Belew, R.K.; Olson, A.J. Automated Docking Using a Lamarckian Genetic Algorithm and an Empirical Binding Free Energy Function. *J. Comput. Chem.* **1999**, *19:14*, 1639-1662. https://doi.org/10.1002/(SICI)1096-987X(19981115)19:14<1639::AID-JCC10>3.0.CO;2-B
42. Neria, E.; Fischer, S.; Karplus, M. Simulation of activation free energies in molecular systems. *J. Chem. Phys.* **1996**, *105*, 1902-1921. https://doi.org/10.1063/1.472061
43. Wang, J.; Wolf, R.M.; Caldwell, J.W.; Kollman, P.A.; Case, D.A. Development and Testing of a General Amber Force Field. *J. Comput. Chem.* **2004**, *25:9*, 1157-1174. https://doi.org/10.1002/jcc.20035
44. Özpinar, G.A.; Peukert, W.; Clark, T. An improved generalized AMBER force field (GAFF) for urea. *J. Mol. Model.* **2016**, *16*, 1427-1440. https://doi.org/10.1007/s00894-010-0650-7
45. Salomon-Ferrer, R.; Case, D.A.; Walker, R.C. An overview of the Amber biomolecular simulation package. *J. Comput. Chem.* **2005**, *26:16*, 1668-1688. https://doi.org/10.1002/jcc.20290
46. Phillips, J.C.; Braun, R.; Wang, W.; Gumbart, J.; Tajkhorshid, E.; Villa, E.; Chipot, C.; Skeel, R.D.; Kalé, L.; Schulten, K. Scalable Molecular Dynamics with NAMD. *J. Comput. Chem.* **2005**, *26:16*, 1781-1802. https://doi.org/10.1002/jcc.20289
47. Phillips, J.C.; Hardy, D.J.; Maia, J.D.C. et al. Scalable molecular dynamics on CPU and GPU architectures with NAMD. *J. Chem. Phys.* **2020**, *153*, 044130. https://doi.org/10.1063/5.0014475
48. Humphrey, W.; Dalke, A.; Schulten, K. VMD: Visual Molecular Dynamics. *J. Mol. Graphics.* **1996**, *14:1*, 33-38. https://doi.org/10.1016/0263-7855(96)00018-5
49. Hayes, J.M.; Archontis, G. MM-GB(PB)SA Calculations of Protein-Ligand Binding Free Energies. Molecular Dynamics - Studies of Synthetic and Biological Macromolecules. **2012**. https://doi.org/10.5772/37107
50. Götz, A.W.; Williamson, M.J.; Xu, D.; Ducan, P.; Grand, S.L.; Walker, R.C.; Routine Microsecond Molecular Dynamics Simulations with AMBER on GPUs. 1. Generalized Born. *J. Chem. Theory. Comput.* **2012**, *8*, 1542-1555. https://doi.org/10.1021/ct200909j
51. Abroshan, H.; Akbarzadeh, H.; Parsafar, G.A. Molecular dynamics simulation and MM–PBSA calculations of sickle cell hemoglobin in dimer form with Val, Trp, or Phe at the lateral contact. *J. Phys. Org. Chem.* **2010**, *23:9*, 866-877. https://doi.org/10.1002/poc.1679

 doi:10.20944/preprints202404.0592.v1



disclaim responsibility for any injury to people or property resulting from any ideas, methods, instructions or products referred to in the content.